Research Article

Electroacupuncture Ameliorates Acute Myocardial Ischemic Injury and Long QT Interval in Mice through the α_{1A}-Adrenergic Receptor: Electrophysiological, Morphological, and Molecular Evidence

Haiyan Zuo [ID],[1] Shuai Cui [ID],[2] Kun Wang [ID],[1] Xin Wu [ID],[2] Jie Zhou [ID],[3] Qiaoyu Qu [ID],[4] Yan Tong [ID],[5] Shengbing Wu [ID],[2,6] and Meiqi Zhou [ID][2,7]

[1]*College of Traditional Chinese Medicine, Anhui University of Chinese Medicine, Hefei City, Anhui Province 230038, China*
[2]*Research Institute of Acupuncture and Meridian, Anhui University of Chinese Medicine, Hefei City, Anhui Province 230038, China*
[3]*Zhejiang Chinese Medical University, Hangzhou City, Zhejiang Province 310053, China*
[4]*Anhui Maternal and Child Health Hospital, Hefei City, Anhui Province 230001, China*
[5]*Xinwu District Hospital of Traditional Chinese Medicine, Wuxi City, Jiangsu Province 214028, China*
[6]*Key Laboratory of Xin'an Medicine, Ministry of Education, Anhui University of Chinese Medicine, Hefei City, Anhui Province 230038, China*
[7]*Bozhou Institute of Chinese Medicine, Anhui Academy of Traditional Chinese Medicine, Bozhou City, Anhui Province 236800, China*

Correspondence should be addressed to Shengbing Wu; wsb922@126.com and Meiqi Zhou; meiqizhou77@sina.com

Acute myocardial ischemia (AMI) is a condition caused by a decrease in blood flow to the heart that can sometimes predispose to acquired long QT syndrome (LQTS), thereby resulting in sudden cardiac death. Recent evidence indicates that electroacupuncture (EA) can alleviate MI injury, but its specific mechanism remains unclear. This study was aimed at investigating the efficacy of EA, which utilizes α_{1A}-adrenergic receptors (α_{1A}-AR) in alleviating MI injury as well as the resulting LQTS. The AMI model was established by ligating the left anterior descending arteries (LAD) of both the wild-type and α_{1A} gene-knockout mice and treating them with EA for three consecutive days. A PowerLab 16 physiological recorder was used to collect the electrocardiogram (ECG) while the serum creatine kinase isoenzymes (CK-MB), lactate dehydrogenase (LDH), and norepinephrine (NE) levels in myocardial tissue were determined by using the enzyme-linked immunosorbent assay (ELISA) kit. Moreover, TTC staining was used to observe the myocardial ischemic area, while H&E and TUNEL staining determined the pathological morphology of the myocardium. Quantitative real-time PCR (qRT-PCR) was used to detect the α_{1A} mRNA, and Western blot was used to detect the specific proteins, such as α_{1A}, cleaved caspase-3, Gq, PLC, p-PKCα, and p-hERG. Our results showed that EA could effectively reduce elevated ST-segment, shorten the extended QT interval, and reduce the serum myocardial enzyme content and the degree of pathological injury in wild mice with MI. EA can also decrease the expression of α_{1A}-AR, PLC, p-PKCα, and NE content in myocardial tissues of wild mice, while those of p-hERG increased in ischemic myocardial tissue. These findings suggested that α_{1A}-AR is involved in the development of MI as well as LQTS. Additionally, EA treatment improves the cardiac function and ischemic long QT interval and plays an important role in reducing the hERG inhibition through the α_{1A}-AR-mediated Gq/PLC/PKCα pathway and myocardial apoptosis. Hence, it is suggested that α_{1A}-AR might become a potential target for EA in treating AMI treatment of myocardial ischemia injury and acquired long QT intervals caused by MI.

1. Introduction

Acute myocardial ischemia (AMI) is a leading cause of death worldwide while its prevalence and mortality rate have been on a steep rise over the past few decades [1, 2]. Ventricular arrhythmias (VA) occur early in ischemia and are regarded as a common cause of sudden death in AMI [3]. Recent clinical evidence indicates that acupuncture can significantly improve the symptoms of angina pectoris in coronary heart disease patients [4, 5]. Therefore, it is of great significance to further explore the role of electroacupuncture (EA) as an effective modality to alleviate AMI injuries.

The KCNH2 gene encodes a voltage-sensitive potassium (K$^+$) channel protein hERG and further mediates the fast activation delay rectifier (K$^+$) channel current (IKr), which plays a major role in cardiac action potential repolarization as well as QT interval adjustment [6]. Furthermore, hERG mutation also impairs the potassium ion channels and induces cell apoptosis as well as endoplasmic reticulum (ER) stress that impacts many cardiac functions [7]. Additionally, the hERG/(IKr) channel inhibition leads to delayed ventricular repolarization and prolonged QT intervals and elicits acquired LQTS [8–11], thus triggering fatal VA [12]. Prolonged QT interval and resting membrane potential (RMP) depolarization during AMI greatly increase the risk of VA and the associated mortality [13, 14]. Corrected QT interval (QTc) based on the Bazett formula can be used as an important risk marker for patients at a higher risk of acute coronary syndrome [15]. Another study confirmed that the blockage of LAD in pigs induced AMI, which in turn prolonged the QTc interval [16]. This suggested that hERG might play a pivotal role in the pathogenesis of AMI injury and acquired LQTS. However, there is little research on the role of hERG in the therapeutic effect of EA against AMI and ischemia-induced long QT interval.

AMI is often accompanied by increased sympathetic nerve activity in conjunction with α_{1A}-AR, which induces arrhythmia [17–19]. The α_{1A}-AR stimulation induces ventricular fibrillation through protein kinase C (PKC) activation during AMI in mouse cardiac tissue [20]. Many previous studies [21, 22] have shown that the α_{1A}-AR activation inhibits cardiac repolarization of hERG/(IKr) current through the PKC pathway. Based on this, it is suggested that the α_{1A}-AR-mediated PKC pathway induces sympathetic nervous system hyperactivity that decreases hERG/(IKr) current, delays ventricular repolarization, and prolongs QT interval, thereby leading to tip torsion and ventricular fibrillation. Therefore, inhibition of α_{1A}-AR and associated signaling pathways and recovery of hERG (K$^+$) channel activity might be effective for shortening the long QT interval after AMI.

In recent years, the effectiveness and safety of acupuncture, as a component of traditional Chinese medicine (TCM), have been recognized for treating ischemic heart diseases [4, 5]. Electroacupuncture (EA) is the application of filiform needles and electrophysiological effects with repetitive frequencies that produce stable stimulation for human acupuncture points [23]. Several in vitro and in vivo experiments reported that acupuncture could improve MI by correcting the abnormalities of ventricular depolarization and repolarization

in mice [24]. Moreover, autonomic nerve activity modulation as a treatment for arrhythmias has been well established in some diseases, such as long QT syndrome [25]. Our previous studies [26–28] confirmed that EA played a protective role in AMI by regulating autonomic nerve activity. Although it is suggested that acupuncture's protective effect might be due to increased expression of K$^+$ channel protein in mice with myocardial infarction [29], the role of EA in improving AMI by regulating α_{1A}-AR and potassium channels as well as shortening the long QT interval is still ambiguous.

Therefore, this study was aimed at exploring the protective effect of EA on the AMI and LQTS as well as at assessing a possible molecular basis for the role of α_{1A}-AR in therapeutic mechanisms of EA for AMI and LQTS.

2. Materials and Methods

2.1. Experimental Animals. Adult male C57 BL/6 mice (aged 8-10 weeks; 18~22 g) were obtained from Zhejiang Hangzhou Ziyuan Experimental Animal Science and Technology Co., Ltd., China. Adult male $\alpha_{1A}{}^{-/-}$ mice (aged 8-10 weeks; 18~22 g) of C57BL/6 genetic background were bred by Jiangsu GemPharmatech Co., Ltd., Nanjing, China, and underwent genotyping using the PCR sequence: P1258 5$'$ CCTGCC TGAATCCATCCG3$'$, P1259 5$'$TTCCCATCA GAATACA AACATCA3$'$, and P1260 5$'$AGCTCCACATG CTCGACTGC3$'$. All mice were kept in environmentally controlled rooms ($22 \pm 2°C$) with a cyclic 12 h light/12 h dark lighting schedule. All mice had free access to food and water. The experimental protocol was approved by the Animal Ethics Committee of Anhui University of Traditional Chinese Medicine (Approval ID AHUCM-2020040).

2.2. Instruments and Reagents. R500 small animal anesthesia machines and disposable acupuncture needles were obtained from Shenzhen Rayward Life Technology Co., Ltd. and Beijing Zhongyan Taihe Medical Instrument Co., Ltd., China, respectively. A PowerLab 16 conductive physiological recorder was from AD Instruments, Australia, while the SDZ-II EA instrument was procured from Suzhou Medical Supplies Factory, China. The following instruments were also used: RM2016 slicer (Shanghai Leica Instrument Co., Ltd., China), optical microscope (Nikon, Japan), RT-600 enzyme marker analyzer (Shenzhen Reddu, China), refrigerated centrifuge (Anhui Jiawen Instrument Equipment Co., Ltd., China), electrophoresis apparatus (BIO-RAD, USA), PS-9 rotary meter (Dalian Jingmai Technology Co., Ltd., China), and an imaging system (Shanghai Tianeng Technology Co., Ltd., China).

The following reagents were utilized: isoflurane (Shenzhen Rayward Life Technology Co., Ltd., China) and CK-MB, LDH, and NE ELISA kit from Shanghai Jianglai Biotechnology Co., Ltd., China. Additionally, the G1501 Tunel Kit was from Wuhan Servicebio, China; anti-cleaved caspase-3 antibody, α_{1A} antibody, anti-PLC antibody, anti-p-PKCα antibody, anti-p-hERG antibody, and β-actin antibody were purchased from Abcam (Cambridge, UK) whereas anti-Gq and sheep anti-rabbit HRP-labeled secondary antibodies were obtained from Novus Biologicals, USA, and Beijing Zhongshan Jinqiao Biotechnology Co., Ltd., China, respectively.

(a)

(b)

(c)

(d)

(e)

(f)

FIGURE 1: Continued.

(g)

(h)

(i)

(j)

(k)

(l)

FIGURE 1: Continued.

(m)

(n)
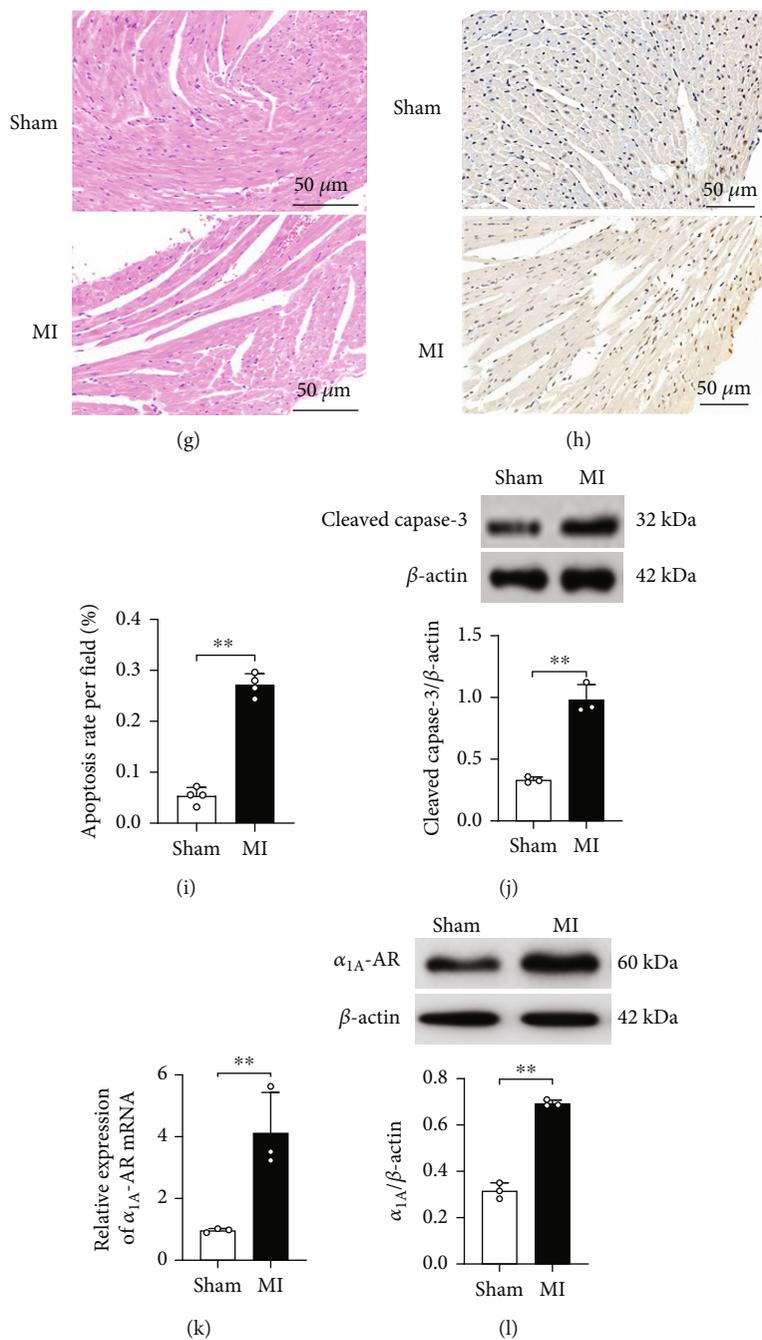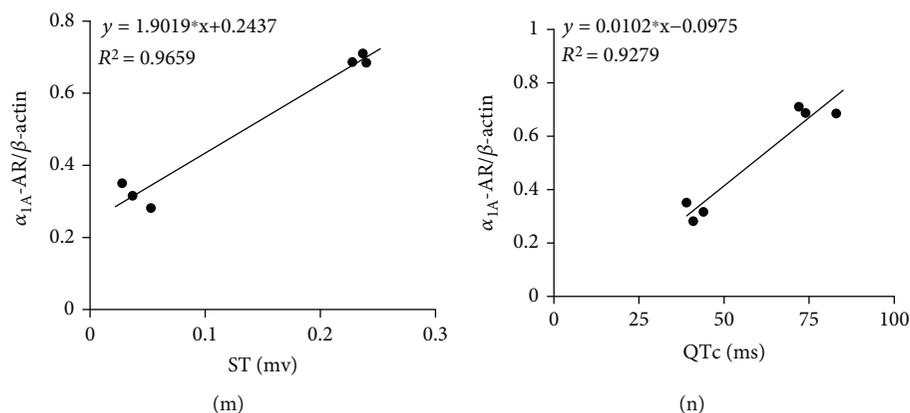
FIGURE 1: MI injury and long QTc interval were associated with an increased α_{1A}-AR expression in the mouse myocardial tissue. ECG showed ST-segment displacement (a, b) and QTc (a, c) after 3 days in MI mice. (d, e) The content of serum myocardial mouse enzymes with MI. (f) The myocardial infarct area was detected by TTC staining. The top figure shows the representative image of TTC staining, and the bottom figure shows the quantitative results of the infarct area. (g) Representative H&E staining of myocardial tissue, magnification: 200x scale bar: 50 μm. (h, i) Representative picture of TUNEL staining and quantitative analysis of myocardial analysis. (j) Western blot images and quantitative analysis of cleaved caspase-3 expression. (k) qRT-PCR quantitatively shows α_{1A} mRNA expression in myocardial tissue. (l) Protein of α_{1A} was analyzed by Western blot. Relative protein expression of α_{1A} and β-actin was used as a control for protein loading. (m, n) Correlation analysis of α_{1A} protein with ST-segment displacement and QTc. Data were presented as mean ± SD. Statistical significance was determined by Student's t-test. $^{**}p < 0.01$.

2.3. Experimental Procedure.

A total of 84 mice, including 48 C57BL/6 wild-type (WT) and 36 $\alpha_{1A}{}^{-/-}$ mice, were randomly divided into seven groups; each group had 12 mice: sham (sham operation), MI, HT7-HT5 (MI+HT7-HT5), LU9-LU8 (MI+LU9-LU8), $\alpha_{1A}{}^{-/-}$+sham, $\alpha_{1A}{}^{-/-}$+MI, and $\alpha_{1A}{}^{-/-}$+MI+HT7-HT5 groups.

The AMI model was established by ligating LAD as described in our previous studies [26–28], whereas LAD was not ligated in the sham group. HT7-HT5 (WT, $\alpha_{1A}{}^{-/-}$) and LU9-LU8 were treated with EA (Shenmen HT7, Tongli HT5, Taiyuan LU9, and Jingqu LU8) the first day after modeling, and the needle was retained for 30 min once a day for three consecutive days. EA adopted the density wave with frequency and intensity of 2 Hz/15 Hz and 1 mA, respectively, while the sham and MI groups received no treatment. Furthermore, all mice were anesthetized by inhaling 5% isoflurane (1 L/min) and were euthanized after blood sampling through orbital venous plexus after three days. After the opening of the thoracic cavity, the hearts were harvested and washed with phosphate-buffered saline (PBS), out of which four hearts were fixed in 4% paraformaldehyde and embedded in paraffin for histological analysis, while the other hearts were stored at −80°C temperature in a refrigerator for subsequent TTC staining, ELISA, Western blot, and qRT-PCR analyses.

2.4. ECG Analysis.

As the mice were anesthetized with 2% isoflurane (1 L/min) and the limbs were fixed, needle electrodes were inserted subcutaneously into the limbs and connected to the PowerLab 16 physiological recorder. The standard II limb ECG of each group was recorded and observed followed by an analysis of the ST-segment and QTc values.

2.5. TTC Staining.

The frozen heart was extracted and sliced into five 1 mm thick slices that were perpendicular to the long axis of the heart and were placed in the prepared 2,3,5-triphenyltetrazole chloride (TTC) staining solution. The oven temperature was maintained at 37°C for 20 min, in a dim environment. Subsequently, the MI area was white while the non-MI area appeared red. ImageJ software was used for processing images after photographic analysis. The myocardial infarct size was calculated by the MI area ratio (%) = white area/total myocardial area * 100%.

2.6. ELISA.

The collected blood samples were allowed to stand at room temperature for one hour and then centrifuged for 15 min (4°C, 3000 r/min) to acquire the supernatant, which was further used for the detection of CK-MB and LDH markers in the mouse serum. The appropriate amount of myocardial tissue homogenate and supernatant was taken for NE detection. The ELISA test was conducted strictly according to the reagent and the kit's instructions.

2.7. Hematoxylin and Eosin (H&E).

After fixation with 4% paraformaldehyde for 24 h, the heart was embedded in paraffin, sliced into 4 μm sections, stained with H&E, and observed under a light microscope.

2.8. TUNEL Assay.

The TUNEL assay detection kit performed the apoptosis assay according to the kit's instructions, in which the positive cells expressed brown color. The percent of apoptotic cells was determined by counting cells in four random fields, in which the percentage of TUNEL positive cells was divided by the number of positive cells by the total number of nuclei in the field.

2.9. qRT-PCR.

The qRT-PCR detected the expression of the α_{1A} gene in the myocardium. Briefly, for purification of total RNA from all the hearts, an animal total RNA rapid extraction kit was used to synthesize cDNA. Real-time PCR was amplified by a 25 μL mixture of SYBR Green Mix (12.5 μL), Primer Mix (0.5 μL), downstream Primer

(a)

(b)

(c)

(d)

(e)

(f)

FIGURE 2: Continued.

(g)

(h)

(i)

(j)
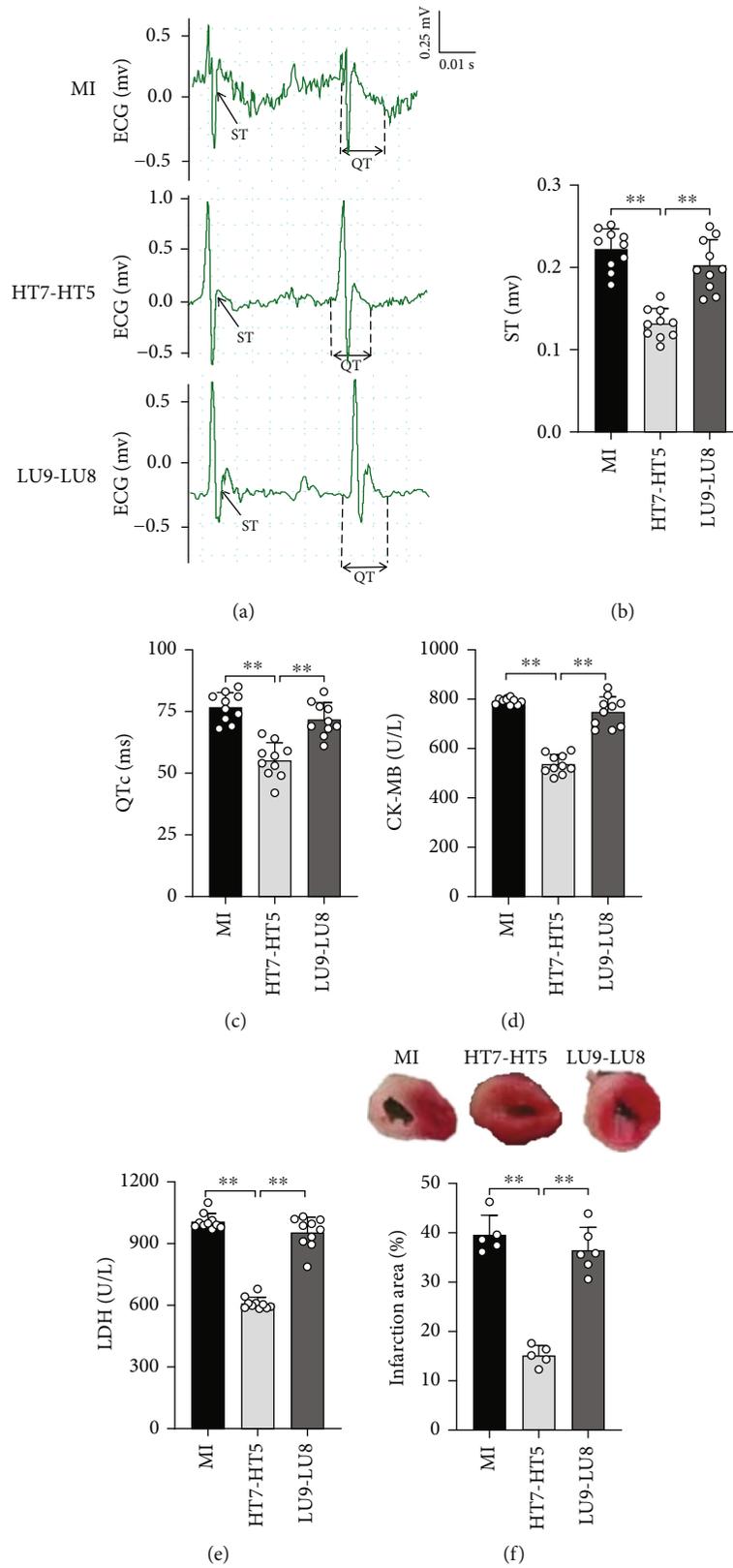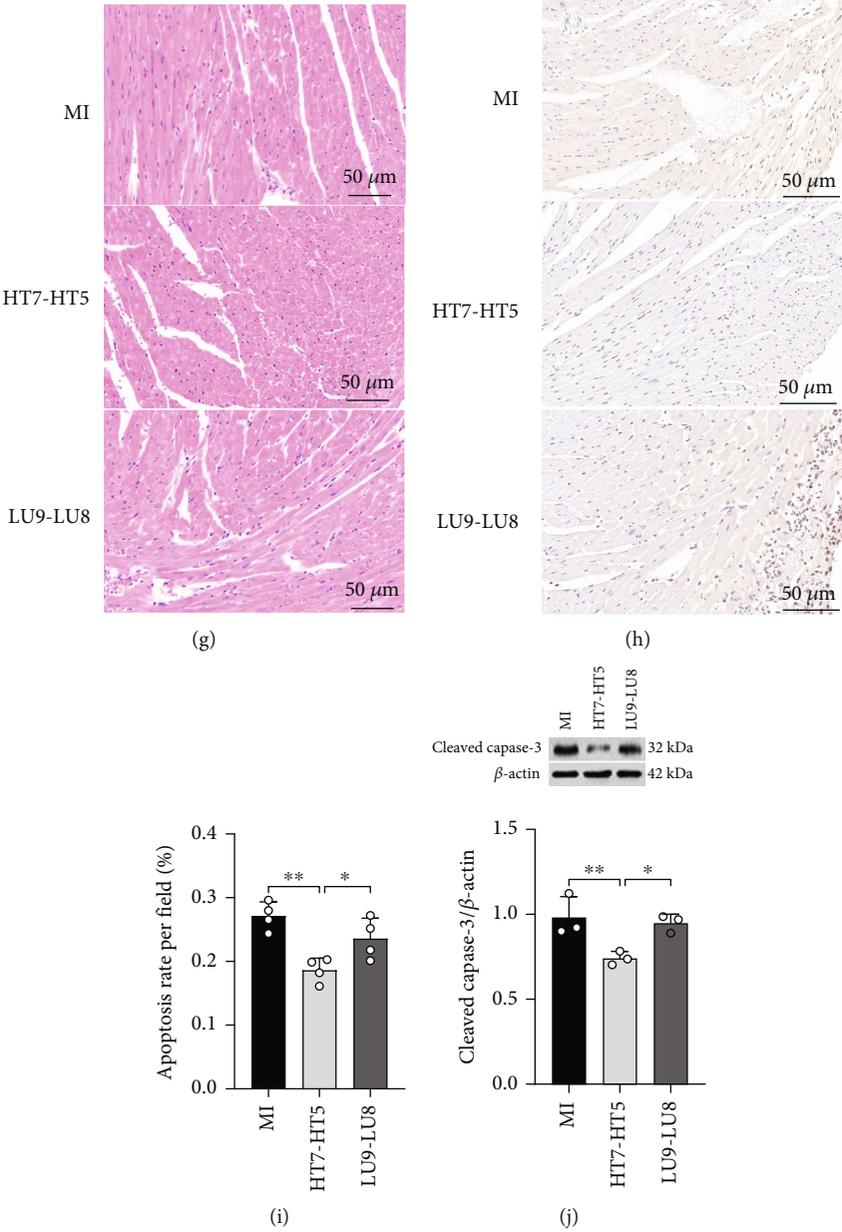
FIGURE 2: Continued.
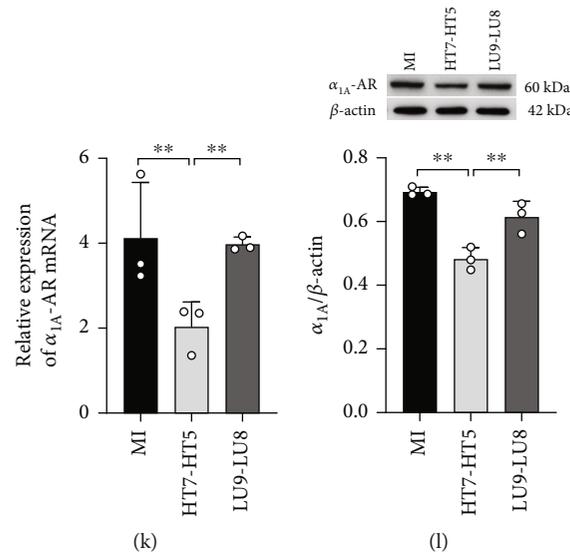
Figure 2: EA alleviates MI injury, shortens LQT interval, and reduces the expression of α_{1A}-AR in myocardial tissue. ECG showed ST-segment displacement (a, b) and QTc (a, c) after 3 days of EA at different acupuncture points in MI mice. (d, e) The content of serum CK-MB and LDH. (f) TTC staining: the top picture shows the TTC staining representative image, and the bottom figure showed the quantitative result of the infarct area. (g) Representative H&E staining of myocardial tissue. Magnifications: 200x; scale bar: 50 μm. (h, i) Representative picture of TUNEL staining and quantification of cardiomyocyte apoptosis. (j) Representative Western blot images showed the protein expression of cleaved caspase-3 in myocardial tissue. (k) Expression of α_{1A} mRNA in mouse myocardial tissue. (l) The protein expression of α_{1A} in myocardial tissue. Data were presented as mean ± SD. One-way ANOVA with the post hoc LSD multiple comparison test. $^{*}p < 0.05$, $^{**}p < 0.01$.

(0.5 μL), ddH$_2$O (9.5 μL), and template mixture (2 μL). The GAPDH antibody was used for normalization, and Premier 5.0 software designed the primer along with the utilized primer sequence: primer F 5′CAAAGCAGGGAGTTTAGT C3′ and primer R 5′GTGAGATGGCTCTGAGTGT3″″.

2.10. Western Blot Analysis.
The myocardial tissue was cut into small fragments, and the lysate was added to the proportion of 150–250 μL lysate per 20 mg of tissue. The purified protein lysate was extracted, and the protein samples were quantified with the BCA protein quantitative reagent. After preparing separation and concentrated gels, an equal amount of total protein was added to each well for electrophoresis and transferred to PVDF membranes which were later immersed in 5% skim milk for one hour and incubated with primary antibodies α_{1A} (1:1000), anti-Gq (1:1000), anti-PLC (1:500), anti-p-PKCα (1:1000), anti-p-hERG (1:10 000), anti-cleaved caspase-3 (1:500), or β-actin (1:5000) at 4°C overnight. Then, the membrane was incubated with a diluted HRP-labeled secondary antibody (1:10000) at 37°C for one hour. The protein bands were observed by using ECL luminescence solution and analyzed by ImageJ software.

2.11. Statistical Analysis.
All experimental data were expressed by mean ± SD and analyzed by SPSS 21.0 software. The histogram was drawn by GraphPad Prism 8.0. The statistical differences between the groups were evaluated by one-way variance analysis (ANOVA), while the post hoc least significant difference (LSD) multiple comparison tests and Student's t-test were used for comparison between the two groups. The difference was considered statistically significant at $^{*}p < 0.05$ and $^{**}p < 0.01$.

3. Results

3.1. MI Injury and Long QTc Interval Were Related to an Increased Expression of α_{1A}-AR in the Myocardium.
To examine the role of α_{1A}-AR in MI and long QTc induced by MI injury, the association between MI and QTc lengthening as well as altered α_{1A} expression in the mouse heart was determined. As shown in Figures 1(a)–1(c), ECG showed ST-segment elevation and QTc interval prolongation in MI mice, while ELISA revealed that the serum CK-MB and LDH contents in MI mice increased significantly (Figures 1(d) and 1(e)). A significant increase in the myocardial ischemic area in the MI group was detected by quantitative TTC staining (Figure 1(f)). H&E staining results showed that the sham group had no abnormal myocardial morphology, whereas the MI group expressed myocardial fiber fracture and inflammatory cell infiltration in the interstitium (Figure 1(g)). TUNEL staining depicted that the apoptosis rate of myocardial cells in the MI group was significantly higher than that in the sham group (Figures 1(h) and 1(i)). The Western blot assay revealed that cleaved caspase-3 protein expression was significantly higher in the MI group when compared with the sham group (Figure 1(j)). In addition, qRT-PCR showed that the expression of α_{1A} mRNA in MI mice was significantly increased after the upregulation of α_{1A} protein (Figures 1(k) and 1(l)). Lastly, the correlation analysis stated that α_{1A} had a positive correlation with MI injury and long QTc (Figures 1(m) and 1(n)). These results suggest that MI and long QTc induced by MI might be associated with abnormal elevation of α_{1A}.

3.2. EA at HT7-HT5 Can Alleviate MI Injury and Long QTc and Decrease the Expression of α_{1A}-AR in MI Mice.
ECG,

(a)

(b)

(c)

(d)
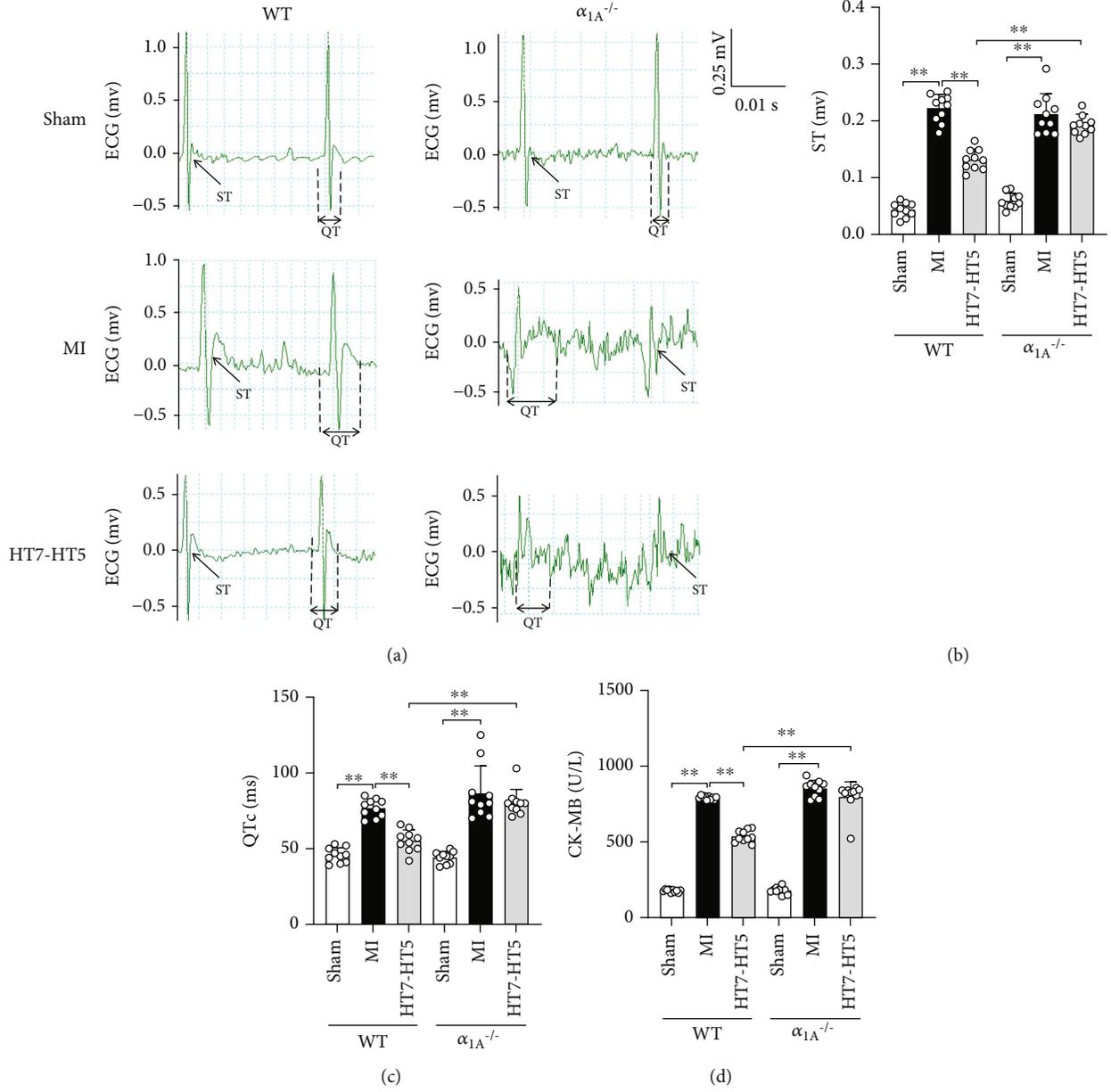
Figure 3: Continued.

(e)

(f)

(g)

(h)

(i)

(j)
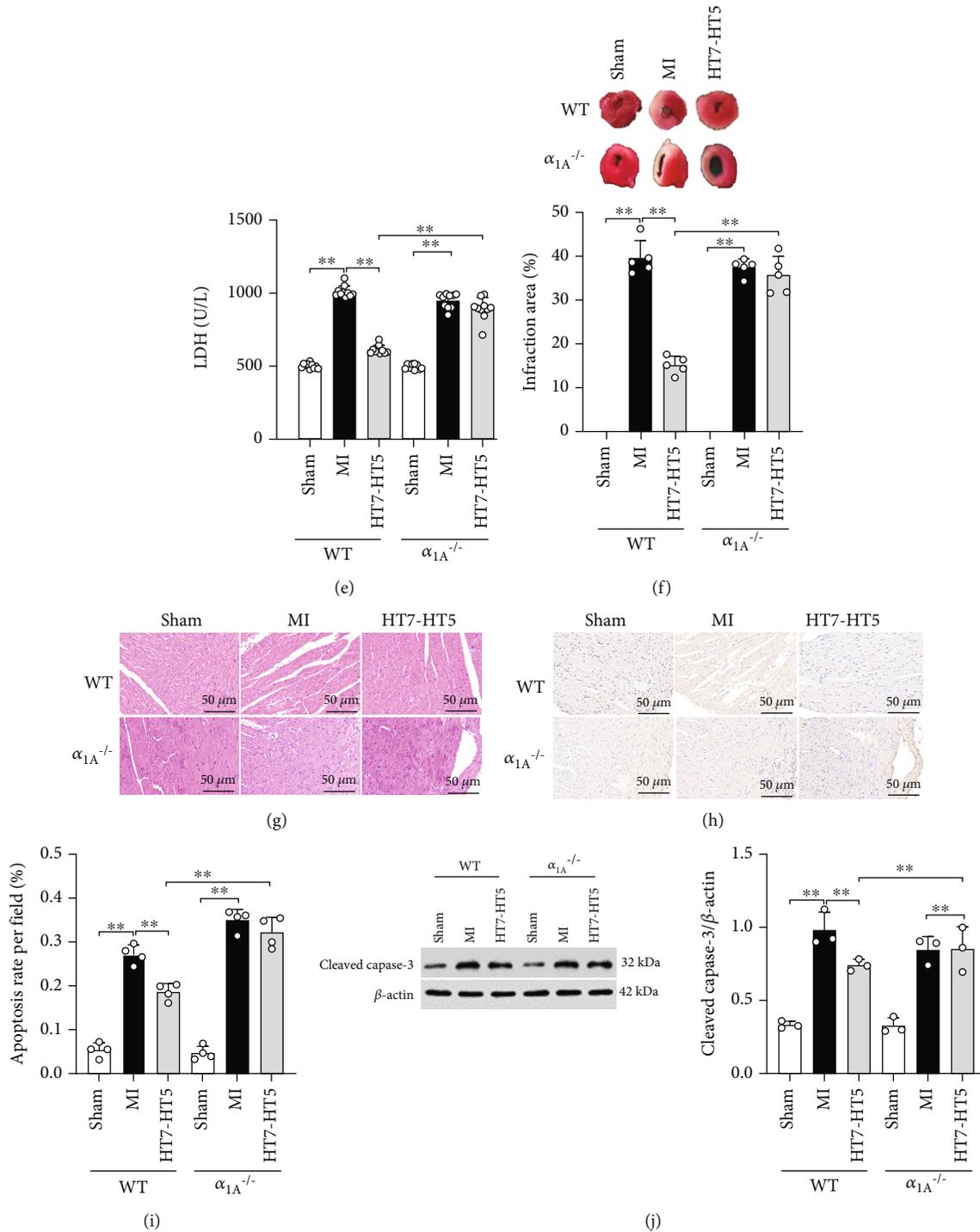
FIGURE 3: The effect of EA on MI injury and long QTc was blocked in $\alpha_{1A}^{-/-}$ mice with MI. (a–c) ECG detection showed ST-segment and QTc interval in mice. (d, e) The content of serum CK-MB and LDH. (f) TTC staining: the top picture shows the TTC staining representative image, and the bottom figure shows the quantitative result of the infarct area. (g) Representative H&E staining of myocardial tissue. Magnification: 200x; scale bar: 50 μm. (h, i) TUNEL staining. The representative picture indicated the apoptosis in cardiomyocytes. The figure shows the quantification of cardiomyocyte apoptosis. Magnification: 200x; scale bar: 50 μm. (j) Protein expression levels of cleaved caspase-3. Data presented are mean ± SD. One-way ANOVA with the post hoc LSD multiple comparison test. $^{*}p < 0.05$, $^{**}p < 0.01$.

histopathological, and Western blot assessments were conducted after EA intervention for 3 days to observe the effects of EA on MI injury, long QTc interval, and α_{1A} expression. As shown in (Figures 2(a)–2(c), ECG showed that the ST segment of the HT7-HT5 group decreased along with the shortening of the QTc interval as compared with the MI and LU9-LU8 groups, whereas ELISA showed that the contents of serum CK-MB and LDH in the HT7-HT5 group
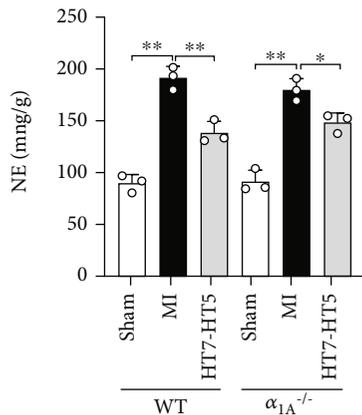
FIGURE 4: NE content in myocardial tissue. Data presented are mean ± SD. One-way ANOVA with the post hoc LSD multiple comparison test. $^*p < 0.05$, $^{**}p < 0.01$.

decreased significantly (Figures 2(d) and 2(e)). TTC staining displayed that the MI area in the HT7-HT5 group was significantly reduced (Figure 2(f)). H&E staining showed broken myocardial fibers along with abundant interstitial infiltration of inflammatory cells in the MI group, whereas myocardial fibers in the HT7-HT5 group were organized and had decreased interstitial inflammatory cell infiltration (Figure 2(g)). TUNEL staining results showed that the apoptosis ratio of myocardial cells in the HT7-HT5 group was significantly reduced when compared to MI and LU9-LU8 groups (Figures 2(h) and 2(i)). The Western blot assay described that the cleaved caspase-3 protein in the HT7-HT5 group was significantly lower than that in the MI and LU9-LU8 groups (Figure 2(j)). In addition, the expression of α_{1A} mRNA and α_{1A} protein was significantly decreased in the HT7-HT5 group when compared with the MI and LU9-LU8 groups (Figures 2(k) and 2(l)). Hence, these results suggest that EA at the HT7-HT5 segment can improve MI injury and long QTc interval than that at the LU9-LU8 segment, and this effect may be related to a decreased α_{1A}-AR expression in myocardial tissue.

3.3. The Cardioprotective Effect of EA at HT7-HT5 Was Significantly Reduced in the $\alpha_{1A}^{-/-}$ Mice.

In order to verify whether α_{1A} deficiency affects the effect of EA on MI injury and long QTc, we prepared $\alpha_{1A}^{-/-}$ mice. As shown in ECG (Figures 3(a)–3(c)), in WT and $\alpha_{1A}^{-/-}$ mice, ST-segment elevation and QTc prolongation in the MI group and the ST-segment and QTc interval of mice in the HT7-HT5 group decreased when compared with the MI group in WT mice. When compared with WT mice, ST-segment and QTc interval of $\alpha_{1A}^{-/-}$ mice did not change significantly when EA was given at HT7-HT5 after MI. The contents of serum CK-MB and LDH significantly decreased after EA at HT7-HT5 under conditions of MI in WT mice (Figures 3(d) and 3(e)). Under the same conditions, the contents of serum CK-MB and LDH in the HT7-HT5 group were not significantly improved in $\alpha_{1A}^{-/-}$ mice (Figures 3(d) and 3(e)). We measured the percentage of the MI area with TTC staining. After MI, the percentage of the ischemic area in $\alpha_{1A}^{-/-}$ mice increased, and the results were similar to those of WT mice

(Figure 3(f)). Our results showed that the MI area in WT mice significantly reduced after EA inception at the HT7-HT5 segment, which was better than that in $\alpha_{1A}^{-/-}$ mice (Figure 3(f)). Next, H&E staining was used to detect myocardial tissue damage. The arrangement of myocardial fibers was organized, and the infiltration of interstitial inflammatory cells decreased after EA at the HT7-HT5 segment under MI conditions in WT mice (Figure 3(g)). As compared to the WT mice, the degree of myocardial tissue injury in $\alpha_{1A}^{-/-}$ mice was not significantly reduced under the same conditions (Figure 3(g)). Furthermore, TUNEL staining showed that the proportion of cardiomyocyte apoptosis in $\alpha_{1A}^{-/-}$ mice was increased (Figures 3(h) and 3(i)), while the expression of the cleaved caspase-3 protein was significantly increased after myocardial infarction, similar to that in WT mice (Figure 3(j)). After EA, the percentage of myocardial cell apoptosis and cleaved caspase-3 protein expression was significantly reduced in WT mice, which was better than that in $\alpha_{1A}^{-/-}$ mice (Figures 3(h)–3(j)). Therefore, $\alpha_{1A}^{-/-}$ mice reversed the protective effect of EA on MI injury and long QTc in mice. These results suggest the potential role of α_{1A}-AR in EA therapy for MI.

3.4. NE in Myocardial Tissue in Mice with MI after EA.

To further confirm the role of α_{1A}, we used ELISA to detect the NE content in WT and $\alpha_{1A}^{-/-}$ mice. As shown in Figure 4, in WT and $\alpha_{1A}^{-/-}$ mice, NE content in myocardial tissue in the MI group significantly increased and was reduced after EA therapy. Our result showed that α_{1A} deficiency did not affect the release of NE. It is suggested that α_{1A}-AR may be a key factor in EA for MI.

3.5. $\alpha_{1A}^{-/-}$ Reversed the Effect of EA on the Gq/PLC/PKCα/hERG Pathway.

In order to explore the mechanism of α_{1A} in inhibiting myocardial infarction injury and long QTc interval after EA, we observed the protein expression levels of Gq, PLC, PKCα, and hERG proteins in myocardial tissue of WT and $\alpha_{1A}^{-/-}$ mice. As seen in Figure 5, Western blot analysis showed that compared with the sham group, the expressions of Gq, PLC, and p-PKCα in myocardial tissue of MI mice significantly increased (Figures 5(a)–5(d)), while the p-hERG expression decreased (Figure 5(e)). The protein expression of Gq, PLC, and PKCα decreased in WT mice after EA, while the p-hERG expression was upregulated. These effects were significantly reduced in $\alpha_{1A}^{-/-}$ mice. These results suggest that EA inhibits hERG through α_{1A}-AR, thereby reducing the activities of Gq, PLC, and PKCα to increase potassium current, accelerate cardiac repolarization, alleviate MI injury, and shorten the long QTc interval. $\alpha_{1A}^{-/-}$ reversed the regulatory effect of EA on Gq/PLC/PKCα and hERG in MI mice.

4. Discussion

Our previous study showed that EA can alleviate MI injury in rats by inhibiting sympathetic hyperexcitation [26, 27]. In this study, EA displayed a protective effect on myocardial tissue morphology and cardiac function, as well as decreasing the long QT interval in MI mice. These beneficial effects
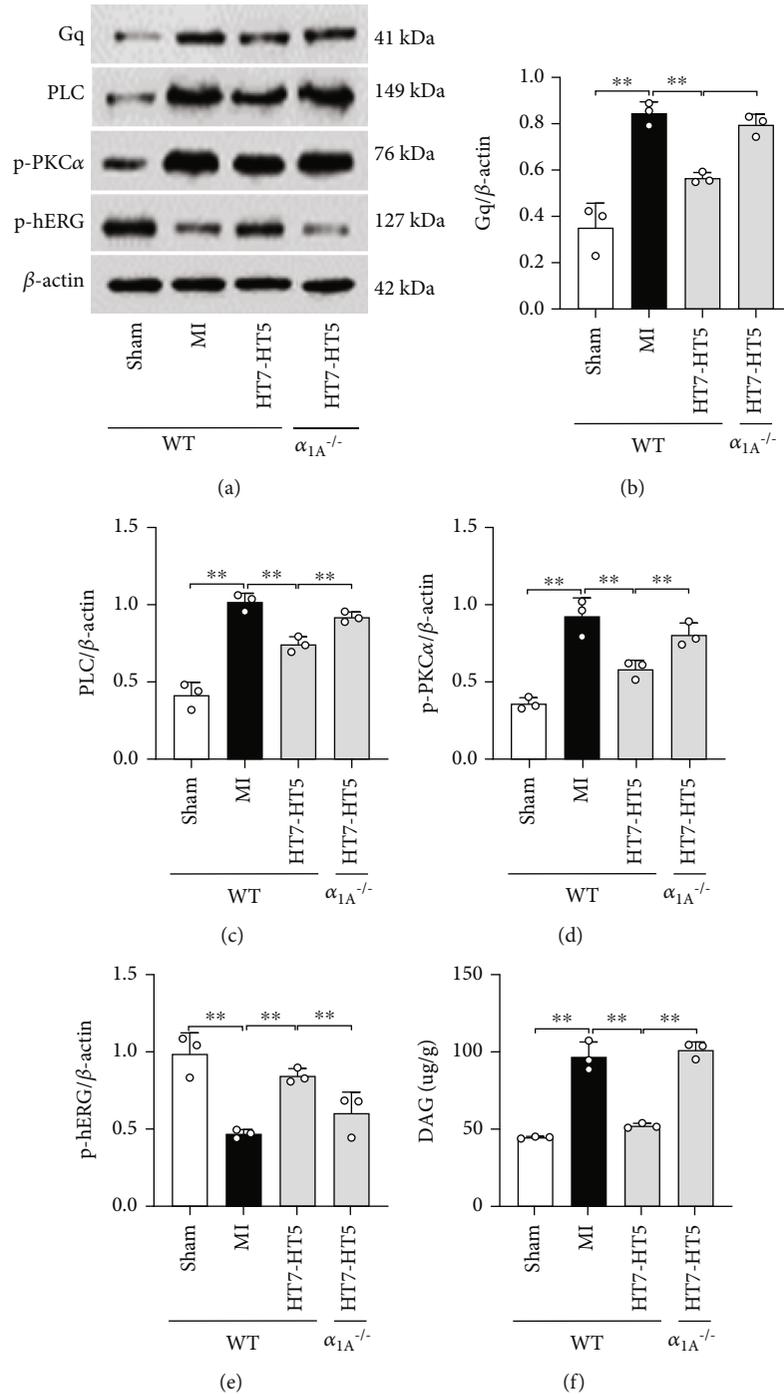
FIGURE 5: $\alpha_{1A}^{-/-}$ reverses the regulation of EA on the Gq/PLC/PKCα pathway and hERG. (a–e) Western blot images showed the protein levels of PLC and the phosphorylation levels of p-PKCα and p-hERG in the mouse myocardium. (f) ELISA showed the DAG content in the mouse myocardium. Data are expressed as mean ± SD. One-way ANOVA with the post hoc LSD multiple comparison test. $^{**}p < 0.01$.

of EA were associated with downregulation and upregulation of α_{1A}-AR and hERG in myocardial tissue, respectively. EA affects the Gq-PLC-PKCα pathway by reducing the hERG channel inhibition by obstructing NE release from sympathetic preganglia. Furthermore, as the α_{1A}-AR stimulation is reduced, the long QT interval gets shortened, and the myocardial injury diminishes. It was observed that α_{1A}-

AR knockout reversed the protective effect of EA on myocardial and long QT intervals in MI mice.

According to a few previous studies, EA can inhibit sympathetic activity and reduce MI injury [27, 28, 30]. It was also discovered that EA activity at the HT7-HT5 point can alleviate MI injury in rats by reducing ST-segment amplitude, serum myocardial enzyme levels, myocardial NE
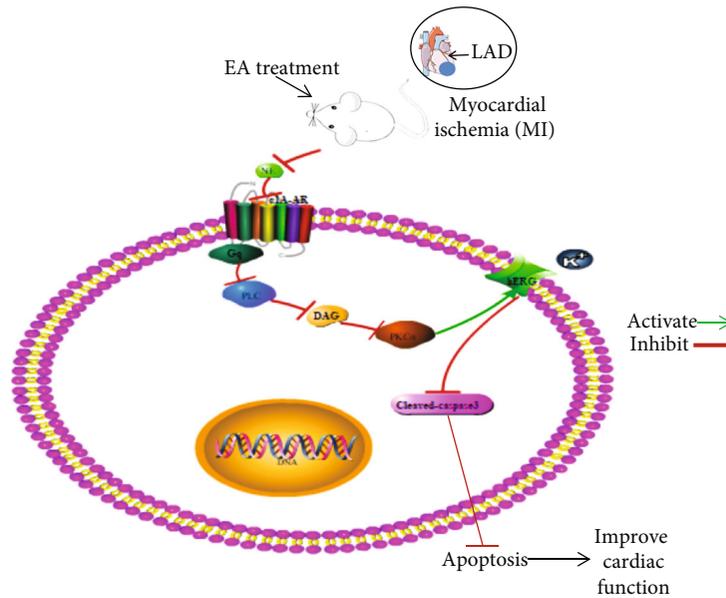
FIGURE 6: The mechanism of α_{1A}-AR-mediated EA in improving MI injury and long QTc interval.

content, and MI area, thus suggesting that EA on hand shaoyin heart meridian points can alleviate MI injury by inhibiting sympathetic nerve excitability [26]. These findings were consistent with our study results. The protective effect of EA on MI is mediated by inhibition of sympathetic activity, and α_{1A}-AR may be involved. A previous study had shown that α_{1A}-AR blockage is beneficial during MI and is consistent with the degree of protection obtained by activating α_1-AR before MI [31]. Therefore, EA might reduce the stimulation of α_{1A}-AR and downstream signal pathways by reducing the NE content of myocardial tissue and the resultant MI injury. However, α_{1A}-AR knockout significantly eliminated the protective effect of EA on MI.

Recent evidence indicates that arrhythmia induced by MI is related to abnormal innervation of cardiac sympathetic nerves [32, 33]. α_{1A}-AR is one of the G protein-coupled receptors (GPCRs), which belongs to the α_1-AR subtype and plays an important role in cardiac physiology and pathology. The α_{1A} activation induced by high sympathetic nerve activity might be an important cause of arrhythmia after MI. A study found that ventricular tachycardia (VT) could be repeatedly stimulated by injecting the α_1 adrenergic agonist phenylephrine into mice [34]. Furthermore, the effect of catecholamine on isolated mouse heart ischemia-induced arrhythmias is mediated mainly by WB 4101-sensitive α_{1A}-AR activation [35]. Since catecholamines induce α_1-AR activation during MI, the increased expression of α_{1A}-AR is closely related to arrhythmia after MI [18, 20, 36, 37]. MI-induced acquired LQTS, characterized by significant changes in QT interval length on ECG, is a prime cause of VA and sudden cardiac death in patients. Corrected QT (QTc) is generally used as an index to predict VA after MI [15, 38, 39]. In our study, it was observed that the QTc value of mice after MI was significantly longer than before, which was consistent with the previous studies [16]. Recent studies suggest that α_{1A}-AR activation reduces cardiac repolariza-

tion K$^+$ current, leading to acquired LQT [40], while the α_1-AR blockers display antiarrhythmic effects in LQT2 animal models, thereby suggesting that α_{1A}-AR might prove to be an effective therapeutic target for acquired LQTS [41]. Pytka et al. suggested that effective α_{1A}-AR blockage is essential to reduce adrenaline-induced arrhythmias [42]. Our results reported that α_{1A} expression increased in mouse myocardial tissue after MI and was proportional to the prolonged QTc value. EA at the HT7-HT5 point can effectively reduce the prolonged QTc value and α_{1A} expression of the myocardium in mice when compared to EA at the LU9-LU8 point. However, these effects are reversed in $\alpha_{1A}^{-/-}$ mice. Therefore, our results suggest that EA might shorten MI-induced long QT intervals by decreasing α_{1A}-AR expression.

The pathogenesis of acquired long LQTS involves hERG channels and fast delay rectifying K$^+$ current (IKr) [43–45]. hERG is voltage-sensitive potassium (K$^+$) channel protein encoded by the KCNH2 gene, which mediates fast delayed rectifying K$^+$ current [46]. Fast delayed rectification K$^+$ current (IKr) plays a key role in cardiac repolarization, and reduced IKr can lead to arrhythmias [6, 47]. The decrease in hERG activity caused by gene mutation, drug inhibition, or MI can reduce IKr and slow ventricular repolarization, thus prolonging QT interval and leading to LQTS [8, 48]. Therefore, hERG activation may become a new pathway for treating acquired LQTS. Activation of α_{1A}-AR has been reported to inhibit cardiac repolarization of hERG/I(Kr) potassium current through the PKC pathway [21, 22]. Liu et al. further demonstrated that PKCα mediated the inhibitory effect of α_{1A} on I(Kr) through the whole-cell patch-clamp technique [40]. However, α_{1A}-AR, in conjunction with Gq, activates downstream molecules and plays an important role in cardiac diseases such as cardiac hypertrophy and arrhythmia [49–52]. It not only regulates the Ca^{2+} processing of cardiomyocytes but also directly changes the

electrophysiological characteristics of the heart [53], which helps in transmembrane signal transduction of α_{1A}-AR [54]. The Gq signal activation triggers PLC activity and hydrolyzes membrane-bound phosphatidylinositol-4,5-diphosphate (PIP2) to form diacylglycerol (DAG); DAG activates PKC and inositol 1,4,5 triphosphate (IP3) and regulates the activity of related ions [55]. PLC-mediated PKC activation has been reported to be associated with the inhibition of time-dependent K^+ current (IKH) by α_{1A}-AR stimulation in atrial fibrillation [56]. Our results showed that Gq, PLC, and p-PKCα protein expressions increased while p-hERG expression decreased with an increased α_{1A}-AR expression in MI mice. EA can inhibit α_{1A}-AR and its downstream signals and upregulate hERG expression to increase cardiac repolarization IKr potassium current and shorten the long QT interval. When α_{1A}-AR was knocked out, the signal regulation of EA weakened, leading to decreased hERG protein expression and the long QTc interval, thus leading to insufficient improvement in MI. This suggests that the improvement of long QT interval by EA treatment depends on the reduction of inhibition of the hERG potassium channel by α_{1A}-AR and downstream Gq-PLC-PKCa signal. Our results are similar to the results from previous studies, which suggested that in HEK293 cells, the intracellular pathways linking α_1-AR to hERG include the activation of Gq, PLC, PIP2, and PKC [22], and PKCα mediates hERG inhibition when α_{1A}-AR is activated [40].

It has been reported that hERG mutations inactivate cell membrane potassium channels and affect the imbalance of Ca^{2+} and Na^+ both inside and outside the cells, leading to cell apoptosis and affecting cardiac structural abnormalities [7]. It has also been found that LQTS mutation can induce apoptosis by activating endoplasmic reticulum stress (ERS). Our results showed that the α_{1A} protein expression was increased, whereas the hERG protein expression decreased in MI mice, and the apoptosis rate was significantly higher than that in the sham group. Furthermore, due to inhibition of α_{1A} by EA, hERG was activated, leading to a reduced expression of cleaved caspase-3 and myocardial cell apoptosis. Previous studies have reported that $\alpha_{1A}^{-/-}$ in mice leads to increased apoptosis and fibrosis of uninfarcted distal cardiomyocytes [57, 58], thus suggesting that α_{1A}-AR is involved in cardiomyocyte survival. In contrast, sustained activation of α_{1A}-AR induced by catecholamines does not benefit the cardiac functions after MI [20, 59, 60]. Taken together, this study further elucidates the protective mechanism of EA on MI and suggests that α_{1A}-AR may be an important molecular target for EA treatment and prevention of MI-induced acquired LQTS and can provide a theoretical basis and experimental support for further studies on EA treatment and rehabilitation of such diseases.

In this study, α_{1A} gene-knockout mice were used to test the effect of EA on MI injury and the relation of LQT interval to α_{1A}-AR expression. The potential limitation of this study is that there was no drug-positive or a negative control group. Considering that EA was only used as in vivo stimulation, the observation of IKr current in mouse cardiomyocytes was not carried out. In future studies, drug control trials and whole-cell patch-clamp techniques should be considered for positive patient outcomes.

5. Conclusion

In conclusion, our results suggest that α_{1A}-AR plays an important role in the EA therapy for MI. EA may upregulate hERG expression by inhibiting the Gq/PLC/PKCα pathway mediated by α_{1A}-AR, shortening the MI-induced LQT interval, reducing the occurrence of ventricular arrhythmias, and ultimately playing a protective role in cardiac function (Figure 6). Our findings further enrich the mechanism of EA treatment for MI injury and acquired LQTs caused by ischemia and provide potential therapeutic modalities for clinical intervention and rehabilitation of such diseases.

Data Availability

The data used to support the findings of this study are available from the corresponding author upon request.

Conflicts of Interest

The authors declared no conflicts of interest.

Authors' Contributions

MQZ conceived and supervised the study. MQZ and HYZ designed the experiments. HYZ, SBW, QYQ, and YT performed the experiments. SC, KW, JZ, and XW analyzed the data. HYZ and MQZ wrote the manuscript. HYZ, SC, and MQZ performed manuscript revisions. All authors reviewed the results and approved the final version of the manuscript. Haiyan Zuo and Shuai Cui have equal contribution.

Acknowledgments

References

[1] R. Gulati, A. Behfar, J. Narula et al., "Acute myocardial infarction in young individuals," *Mayo Clinic Proceedings*, vol. 95, no. 1, pp. 136–156, 2020.

[2] M. Zhou, H. Wang, X. Zeng et al., "Mortality, morbidity, and risk factors in China and its provinces, 1990–2017: a systematic analysis for the Global Burden of Disease Study 2017," *Lancet*, vol. 394, no. 10204, pp. 1145–1158, 2019.

[3] J. Bhar-amato, W. Davies, and S. Agarwal, "Ventricular arrhythmia after acute myocardial infarction the perfect storm," *Arrhythmia & electrophysiology review*, vol. 6, no. 3, pp. 134–139, 2017.

[4] L. Zhao, D. Li, H. Zheng et al., "Acupuncture as adjunctive therapy for chronic stable angina," *JAMA Internal Medicine*, vol. 179, no. 10, pp. 1388–1397, 2019.

[5] J. S. Wang, X. D. Yu, S. Deng, H. W. Yuan, and H. S. Li, "Acupuncture on treating angina pectoris: a systematic review," *Medicine (Baltimore)*, vol. 99, no. 2, p. e18548, 2020.

[6] A. Butler, M. V. Helliwell, Y. Zhang, J. C. Hancox, and C. E. Dempsey, "An update on the structure of hERG," *Frontiers in pharmacology*, vol. 10, p. 1572, 2019.

[7] Y. Z. Shuting Ma, M. M. Cao, and C. F. Sun, "Human ether-à-go-go-related gene mutation L539fs/47-hERG leads to cell apoptosis through the endoplasmic reticulum stress pathway," *International Journal of Molecular Medicine*, vol. 43, pp. 1253–1262, 2019.

[8] D. K. Jones, F. Liu, R. Vaidyanathan, L. L. Eckhardt, M. C. Trudeau, and G. A. Robertson, "hERG 1b is critical for human cardiac repolarization," *Proceedings of the National Academy of Sciences*, vol. 111, no. 50, pp. 18073–18077, 2014.

[9] H. Nogawa and T. Kawai, "hERG trafficking inhibition in drug-induced lethal cardiac arrhythmia," *European Journal of Pharmacology*, vol. 741, pp. 336–339, 2014.

[10] D. K. Jones, A. C. Johnson, E. C. Roti Roti et al., "Localization and functional consequences of a direct interaction between TRIOBP-1 and hERG/KCNH2 proteins in the heart," *Journal of cell science*, vol. 131, no. 6, p. jcs206730, 2018.

[11] X. Dong, Y. Liu, H. Niu et al., "Electrophysiological characterization of a small molecule activator on human ether-a-go-go-related gene (hERG) potassium channel," *Journal of Pharmacological Sciences*, vol. 140, no. 3, pp. 284–290, 2019.

[12] L. X. Cubeddu, "QT prolongation and fatal arrhythmias: a review of clinical implications and effects of drugs," *American Journal of Therapeutics*, vol. 10, pp. 452–457, 2003.

[13] K. E. Sandau, M. Funk, A. Auerbach et al., "Update to practice standards for electrocardiographic monitoring in hospital settings: a scientific statement from the American Heart Association," *Circulation*, vol. 136, no. 19, pp. e273–e344, 2017.

[14] Z. Li, Q. He, C. Wu et al., "Apelin shorten QT interval by inhibiting $Kir2.1/IK1$ via a PI3K way in acute myocardial infarction," *Biochemical and Biophysical Research Communications*, vol. 517, no. 2, pp. 272–277, 2019.

[15] M. Nabati, Z. Dehghan, B. Kalantari, and J. Yazdani, "Corrected QT interval prolongations in patients with non–ST-elevation acute coronary syndrome," *The Journal of Tehran University Heart Center*, vol. 13, no. 4, pp. 173–179, 2018.

[16] S. S. Kim, H. K. Kim, H. W. Park et al., "Effect of renal denervation on suppression of PVC and QT prolongation in a porcine model of acute myocardial infarction," *Korean Circulation Journal*, vol. 50, no. 1, pp. 38–49, 2020.

[17] E. P. Anyukhovsky and M. R. Rosen, "Abnormal automatic rhythms in ischemic purkinje fibers are modulated by a specific alpha 1-adrenergic receptor subtype," *Circulation*, vol. 83, pp. 2076–2082, 1991.

[18] R. Tölg, T. Kurz, M. Ungerer, J. Schreieck, B. Görge, and G. Richardt, "Influence of alpha-and beta-adrenoceptor antagonists on ventricular fibrillation in ischemic rat hearts," *Naunyn-Schmiedeberg's archives of pharmacology*, vol. 356, pp. 62–68, 1997.

[19] M. Kleine-Brueggeney, I. Gradinaru, E. Babaeva, D. A. Schwinn, and A. Oganesian, "Alpha1a-adrenoceptor genetic variant induces cardiomyoblast-to-fibroblast-like cell transition via distinct signaling pathways," *Cellular Signalling*, vol. 26, no. 9, pp. 1985–1997, 2014.

[20] R. Tölg, J. Schreieck, T. Kurz, H. A. Katus, and G. Richardt, "Ischemia-induced ventricular fibrillation in isolated perfused rat heart: role of alpha1A-adrenoceptor mediated activation of protein kinase C," *Basic Research in Cardiology*, vol. 96, no. 1, pp. 68–74, 2001.

[21] D. Thomas, K. Wu, A. B. Wimmer et al., "Activation of cardiac human ether-a-go-go related gene potassium currents is regulated by α1A-adrenoceptors," *Journal of Molecular Medicine (Berlin, Germany)*, vol. 82, no. 12, pp. 826–837, 2004.

[22] J. Urrutia, A. Alday, M. Gallego et al., "Mechanisms of IhERG/IKr modulation by α1-adrenoceptors in HEK293 cells and cardiac myocytes," *Cellular Physiology and Biochemistry*, vol. 40, no. 6, pp. 1261–1273, 2016.

[23] N. Ding, Q. Wei, W. Deng, X. Sun, J. Zhang, and W. Gao, "Electroacupuncture alleviates inflammation of dry eye diseases by regulating the α7nAChR/NF-κB signaling pathway," *Oxidative Medicine and Cellular Longevity*, vol. 2021, Article ID 6673610, 15 pages, 2021.

[24] J. Tang, W. Ren, Y. Liu, H. Gao, Y. Wang, and S. Huang, "Effects of post-treatment electroacupuncture on ventricular monophasic action potential and cardiac function in a rat model of ischemia/reperfusion injury," *Acupuncture in Medicine*, vol. 40, no. 1, pp. 89–98, 2022.

[25] L. P. Qin, J. H. Gao, W. X. Fu et al., "Effects of electroacupuncture pretreatment on ischemic arrhythmia and intracellular calcium oscillation in single cardiocyte isolated from rats with myocardial ischemia and reperfusion," *Zhen Ci Yan Jiu*, vol. 33, no. 2, pp. 75–79, 2008.

[26] X. Wu, K. Wang, S. Cui, S. Wu, G. Zhu, and M. Zhou, "Electroacupuncture ameliorates acute myocardial ischemia: a potential role of the locus coeruleus," *Evidence-Based Complementary and Alternative Medicine*, vol. 2020, Article ID 4298657, 12 pages, 2020.

[27] S. Cui, Y. Zhou, S. Wu, J. Cao, G. Zhu, and M. Zhou, "Electroacupuncture improved the function of myocardial ischemia involved in the hippocampus-paraventricular nucleus-sympathetic nerve pathway," *Evidence-Based Complementary and Alternative Medicine*, vol. 2018, Article ID 2870676, 13 pages, 2018.

[28] S. Cui, J. Xu, J. Wang, S. B. Wu, Y. P. Zhou, and M. Q. Zhou, "Effect of electroacupuncture stimulation of heart meridian on autonomic nervous activities in acute myocardial ischemia rats," *Zhen Ci Yan Jiu*, vol. 41, no. 6, pp. 515–520, 2016.

[29] W. S. Zhao, D. Li, Y. H. Xu et al., "The beneficial effects of electroacupuncture at PC6 acupoints (Neiguan) on myocardial ischemia in ASIC3 −/− mice," *Journal of Acupuncture and Meridian Studies*, vol. 11, no. 3, pp. 88–96, 2018.

[30] X. Cui, H. L. Cao, Q. Liu, K. Liu, X. Y. Gao, and B. Zhu, "Electroacupuncture at "Neiguan" (PC6) decreased cardiac sympathetic hyperactivity and improved cardiac function in chronic myocardial ischemia model rats," *Zhen Ci Yan Jiu*, vol. 45, no. 4, pp. 264–268, 2020.

[31] M. Loubani and M. Galinanes, "Alpha 1-adrenoceptors during simulated ischemia and reoxygenation of the human myocardium: effect of the dose and time of administration," *The Journal of Thoracic and Cardiovascular Surgery*, vol. 122, no. 1, pp. 103–112, 2001.

[32] T. Sasano, M. R. Abraham, K. C. Chang et al., "Abnormal sympathetic innervation of viable myocardium and the substrate of ventricular tachycardia after myocardial infarction," *Journal of the American College of Cardiology*, vol. 51, no. 23, pp. 2266–2275, 2008.

[33] R. Lautamaki, T. Sasano, T. Higuchi et al., "Multiparametric molecular imaging provides mechanistic insights into sympathetic innervation impairment in the viable infarct border zone," *Journal of Nuclear Medicine*, vol. 56, no. 3, pp. 457–463, 2015.

[34] E. Kurtzwald-Josefson, E. Hochhauser, K. Bogachenko et al., "Alpha blockade potentiates CPVT therapy in calsequestrin-mutant mice," *Heart Rhythm*, vol. 11, no. 8, pp. 1471–1479, 2014.

[35] P. M. L. Janssen, B. D. Canan, A. Kilic, B. A. Whitson, and A. J. Baker, "Human myocardium has a robust α1A-subtype adrenergic receptor inotropic response," *Journal of Cardiovascular Pharmacology*, vol. 72, no. 3, pp. 136–142, 2018.

[36] A. D. Ivanova, T. S. Filatova, D. V. Abramochkin et al., "Attenuation of inward rectifier potassium current contributes to the alpha 1-adrenergic receptor-induced proarrhythmicity in the caval vein myocardium," *Acta Physiologica*, vol. 231, no. 4, article e13597, 2021.

[37] M. Y. A. M. Avkiran, "Exacerbation of reperfusion arrhythmias by alpha 1 adrenergic stimulation a potential role for receptor mediated activation of sarcolemmal sodium-hydrogen exchange," *Cardiovascular research*, vol. 29, pp. 222–230, 1995.

[38] M. Hetland, K. H. Haugaa, S. I. Sarvari, G. Erikssen, E. Kongsgaard, and T. Edvardsen, "A novel ECG-index for prediction of ventricular arrhythmias in patients after myocardial infarction," *Annals of Noninvasive Electrocardiology*, vol. 19, no. 4, pp. 330–337, 2014.

[39] I. Stankovic, B. Putnikovic, A. Janicijevic et al., "Myocardial mechanical and QTc dispersion for the detection of significant coronary artery disease," *European Heart Journal Cardiovascular Imaging*, vol. 16, no. 9, pp. 1015–1022, 2015.

[40] X. Liu, Y. Wang, H. Zhang, L. Shen, and Y. Xu, "Different protein kinase C isoenzymes mediate inhibition of cardiac rapidly activating delayed rectifier K+ current by different G-protein coupled receptors," *British Journal of Pharmacology*, vol. 174, no. 23, pp. 4464–4477, 2017.

[41] T. Mow, K. Frederiksen, M. B. Thomsen, and M. B. Thomsen, "Assessment of anti-arrhythmic activity of antipsychotic drugs in an animal model: Influence of non-cardiac α1-adrenergic receptors," *European Journal of Pharmacology*, vol. 748, pp. 10–17, 2015.

[42] K. Pytka, K. Lustyk, E. Żmudzka et al., "Chemically homogenous compounds with antagonistic properties at all α1-adrenoceptor subtypes but not β1-adrenoceptor attenuate adrenaline-induced arrhythmia in rats," *Frontiers in Pharmacology*, vol. 7, p. 229, 2016.

[43] S. M. Lamothe, J. Guo, W. Li, T. Yang, and S. Zhang, "The human ether-a-go-go-related gene (hERG) potassium channel represents an unusual target for protease-mediated damage," *The Journal of Biological Chemistry*, vol. 291, no. 39, pp. 20387–20401, 2016.

[44] S. M. Lamothe, W. Song, J. Guo et al., "Hypoxia reduces mature hERG channels through calpain up-regulation," *The FASEB Journal*, vol. 31, no. 11, pp. 5068–5077, 2017.

[45] N. Zemzemi and B. Rodriguez, "Effects of L-type calcium channel and human ether-a-go-go related gene blockers on the electrical activity of the human heart: a simulation study," *Europace*, vol. 17, no. 2, pp. 326–333, 2015.

[46] N. Chiamvimonvat, Y. Chen-Izu, C. E. Clancy et al., "Potassium currents in the heart: functional roles in repolarization, arrhythmia and therapeutics," *The Journal of Physiology*, vol. 595, no. 7, pp. 2229–2252, 2017.

[47] J. I. Vandenberg, M. D. Perry, M. J. Perrin, S. A. Mann, Y. Ke, and A. P. Hill, "hERG K+ channels: structure, function, and clinical significance," *Physiological Reviews*, vol. 92, no. 3, pp. 1393–1478, 2012.

[48] J. M. Kratz, U. Grienke, O. Scheel, S. A. Mann, and J. M. Rollinger, "Natural products modulating the hERG channel: heartaches and hope," *Natural Product Reports*, vol. 34, no. 8, pp. 957–980, 2017.

[49] C. Park-Windhol, P. Zhang, M. Zhu et al., "Gq/11-mediated signaling and hypertrophy in mice with cardiac-specific transgenic expression of regulator of G-protein signaling 2," *PLOS One*, vol. 7, no. 7, p. 40048, 2012.

[50] K. Wiesen, E. Kaiser, L. Schröder et al., "Cardiac remodeling in Galphaq and Galpha11 knockout mice," *International Journal of Cardiology*, vol. 202, pp. 836–845, 2016.

[51] A. Tinker, M. Finlay, M. Nobles, and A. Opel, "The contribution of pathways initiated via the Gq\11 G-protein family to atrial fibrillation," *Pharmacological research*, vol. 105, pp. 54–61, 2016.

[52] N. Matsushita, T. Kashihara, H. Shimojo et al., "Cardiac overexpression of constitutively active Galpha q causes angiotensin II type1 receptor activation, leading to progressive heart failure and ventricular arrhythmias in transgenic mice," *PLOS One*, vol. 9, no. 8, p. e106354, 2014.

[53] E. Kaiser, Q. Tian, M. Wagner et al., "DREADD technology reveals major impact of Gq signalling on cardiac electrophysiology," *Cardiovascular Research*, vol. 115, no. 6, pp. 1052–1066, 2019.

[54] B. E. Myagmar, T. Ismaili, P. M. Swigart et al., "Coupling to Gq signaling is required for cardioprotection by an alpha-1A-adrenergic receptor agonist," *Circulation Research*, vol. 125, no. 7, pp. 699–706, 2019.

[55] D. Kamato, P. Mitra, F. Davis et al., "Gaq proteins: molecular pharmacology and therapeutic potential," *Cellular and Molecular Life Sciences*, vol. 74, no. 8, pp. 1379–1390, 2017.

[56] Y. H. Yeh, J. R. Ehrlich, X. Qi, T. E. Hébert, D. Chartier, and S. Nattel, "Adrenergic control of a constitutively active acetylcholine-regulated potassium current in canine atrial cardiomyocytes," *Cardiovascular Research*, vol. 74, no. 3, pp. 406–415, 2007.

[57] Y. Huang, C. D. Wright, C. L. Merkwan et al., "An α1A-adrenergic–extracellular signal-regulated kinase survival signaling pathway in cardiac myocytes," *Circulation*, vol. 115, no. 6, pp. 763–772, 2007.

[58] C. C. Yeh, Y. Fan, Y. Xu, Y. L. Yang, P. C. Simpson, and M. J. Mann, "Shift toward greater pathologic post-myocardial infarction remodeling with loss of the adaptive hypertrophic signaling of alpha1 adrenergic receptors in mice," *PLOS One*, vol. 12, no. 12, p. e0188471, 2017.

[59] K. Suita, T. Fujita, N. Hasegawa et al., "Norepinephrine-induced adrenergic activation strikingly increased the atrial fibrillation duration through beta1-and alpha1-adrenergic receptor-mediated signaling in Mice," *PLOS One*, vol. 10, no. 7, p. e0133664, 2015.

[60] H. Chaulet, F. Lin, J. Guo et al., "Sustained augmentation of cardiac α1A-adrenergic drive results in pathological remodeling with contractile dysfunction, progressive fibrosis and reactivation of matricellular protein genes," *Journal of Molecular and Cellular Cardiology*, vol. 40, no. 4, pp. 540–552, 2006.